BCS-BEC crossover in spin-orbit-coupled two-dimensional Fermi gases

Gang Chen, Ming Gong, and Chuanwei Zhang

Phys. Rev. A **85**, 013601 — Published 3 January 2012

DOI: 10.1103/PhysRevA.85.013601

BCS-BEC crossover in spin-orbit coupled two-dimensional Fermi gases

Gang Chen,[1, 2, 3] Ming Gong,[1] and Chuanwei Zhang[1, *]

[1] *Department of Physics and Astronomy, Washington State University, Pullman, Washington, 99164 USA*
[2] *Department of Physics, Shaoxing University, Shaoxing 312000, P. R. China*
[3] *State Key Laboratory of Quantum Optics and Quantum Optics Devices, College of Physics and Electronic Engineering, Shanxi University, Taiyuan 030006, P. R. China*

The recent experimental realization of spin-orbit coupling for ultra-cold atoms has generated much interest in the physics of spin-orbit coupled degenerate Fermi gases. Although recently the BCS-BEC crossover in three-dimensional (3D) spin-orbit coupled Fermi gases has been intensively studied, the corresponding two-dimensional (2D) crossover physics has remained unexplored. In this paper, we investigate, both numerically and analytically, the BCS-BEC crossover physics in 2D degenerate Fermi gases in the presence of a Rashba type of spin-orbit coupling. We derive the mean field gap and atom number equations suitable for the 2D spin-orbit coupled Fermi gases and solve them numerically and self-consistently, from which the dependence of the ground state properties (chemical potential, superfluid pairing gap, ground state energy per atom) on the system parameters (e.g., binding energy, spin-orbit coupling strength) is obtained. Furthermore, we derive analytic expressions for these ground state quantities, which agree well with our numerical results within a broad parameter region. Such analytic expressions also agree qualitatively with previous numerical results for the 3D spin-orbit coupled Fermi gases, where analytic results are lacked. We show that with an increasing SOC strength, the chemical potential is shifted by a constant determined by the SOC strength. The superfluid pairing gap is enhanced significantly in the BCS limit for strong SOC, but only increases slightly in the BEC limit.

PACS numbers: 03.75.Ss, 05.30. Fk, 74.20.Fg

I. INTRODUCTION

Spin-orbit coupling (SOC), the interaction between the spin and orbital degrees of freedom of a particle, has played important roles in condensed matter as well as atomic and nuclear physics. For instance, it is known that the coupling between electron spin and its linear momentum in solids leads to many important condensed matter phenomena such as spin and anomalous Hall effects [1, 2], topological insulators and and superconductors [3], spintronics [4], *etc.* In atomic physics, the coupling between the electron spin and its motion around an atomic nucleus is responsible for many of the details of atomic structure [5].

Superfluidity and superconductivity are another important phenomena in physics and have been widely studied in many physical systems, including solids, Helium liquids, as well as ultra-cold atomic gases [6]. Although particles in superfluids and superconductors usually possess spins or pseudospins, the effects of SOC on superfluidity and superconductivity have remained largely unexplored. In this context, the recent experimental realization of SOC for ultra-cold atoms [7] provides a completely new platform for exploring many-body phenomena in spin-orbit coupled superfluids, including both Bose-Einstein condensates (BECs) [8, 9] and degenerate Fermi gases [10, 11]. In the presence of SOC, various new and exotic superfluid phenomena may exist since spins are not conserved during their motion. In particular, in spin-orbit coupled BECs, the ground state phase diagrams as well as the collective excitations have been studied [8]. In spin-orbit coupled degenerate Fermi gases, the crossover physics from the Bardeen-Cooper-Schrieffer (BCS) superfluids of loosely bounded Cooper pairs to the BEC of tightly bounded molecules has been investigated extensively, in both uniform and trapped three-dimensional (3D) gases [10, 11]. However, the study of spin-orbit coupled two-dimensional (2D) Fermi gases is still lacked.

On the other hand, the 2D degenerate Fermi gas (without SOC) in itself is one of the most active topics in ultra-cold atomic physics [12]. Experimentally, the 2D degenerate Fermi cold atomic gases have been realized recently using a highly anisotropic pancake-shaped potential [13], and the interaction energy in this system has been measured using the radio-frequency spectroscopy [14]. In this system, tunable interactions between atoms through Feshbach resonance [15] allow the exploration of the crossover physics from the BCS superfluids to the BEC of molecules in 2D [16]. In addition to the study of many-body physics such as quantum fluctuations, non-Fermi liquid behavior, etc. [17], the 2D Fermionic cold atomic gases are particularly interesting because of the existence of exotic topological excitations such as Majorana fermions with non-Abelian exchange statistics [18].

Motivated by these recent experimental breakthroughs in the realization of SOC and 2D Fermi gases, in this paper, we investigate, both numerically and analytically, the BCS-BEC crossover physics in 2D degenerate Fermi gases in the presence of a Rashba type of SOC. Our main

*Electronic address: cwzhang@wsu.edu

results are the following:

1) We derive the mean field gap and atom number equations suitable for the 2D spin-orbit coupled Fermi gases.

2) These two equations are solved numerically and self-consistently, from which the dependence of the ground state properties (chemical potential, superfluid pairing gap, ground state energy per atom) on the system parameters (e.g., binding energy, SOC strength) is obtained.

3) We derive analytic expressions for these ground state physical quantities, which agree well with our numerical results within a broad parameter region. Such analytic expressions also agree qualitatively with previous numerical results for the 3D spin-orbit coupled Fermi gases [10], where analytic results are lacked.

4) We find that with an increasing SOC strength α, the chemical potential is shifted by a constant $-m\alpha^2$ determined by α. The superfluid pairing gap and the ground state energy per atom are affected at the order of α^4 rather than α^2, which means that weak SOC does not affect the pairing gap and the ground state energy per atom. In the strong SOC regime, the pairing gap and the ground state energy are enhanced significantly in the BCS limit, but only increase slightly in the BEC limit. Although these analytic results are obtained for the 2D Fermi gases, they also provide qualitative understanding for the numerical results in 3D Fermi gases [10], where similar changes of the chemical potential and superfluid pairing order with respect to the SOC strength are observed but analytic results are lacked.

The paper is organized as follows. Section II describes the physical system: the spin-orbit coupled 2D degenerate Fermi gases, and the corresponding Hamiltonian. In section III, we derive the mean field gap and atom number equations. These equations are self-consistently solved in section IV, both numerically and analytically (through perturbative methods), to obtain the ground state properties (chemical potential, superfluid order parameter, and ground state energy per atom) of the spin-orbit coupled Fermi gases in the BCS-BEC crossover. Section V consists of discussion and conclusion.

II. THE PHYSICAL SYSTEM AND THE HAMILTONIAN

The physical system in consideration is a 2D degenerate Fermi gas. Experimentally, the 2D degenerate Fermi gas has been realized using a 1D deep optical lattice along the third dimension, where the tunneling between different layers is suppressed completely [13, 14]. The 1D optical lattice potential $V_0 \sin^2(2\pi z/\lambda_w)$ can be generated using two counter-propagating laser beams (parallel to the z axis with a wavelength λ_w). In this case, the two-body binding energy is given by $E_b \simeq 0.915\hbar\omega_L \exp(\sqrt{2\pi} l_L/a_s)/\pi$, where $\omega_L = \sqrt{8\pi^2 V_0/(m\lambda_w^2)}$ is the effective trapping frequency along the z axis, $l_L = \sqrt{\hbar/(m\omega_L)}$, and a_s is the 3D s-wave scattering length [19]. Therefore the two-body binding energy E_b can be tuned by varying the s-wave scattering length a_s via the Feshbash resonance for the study of the BCS-BEC crossover physics [16]. For a small attractive $a_s \to 0^-$, $E_b \to 0$, corresponding to the BCS limit. While for a small repulsive $a_s \to 0^+$, $E_b \to \infty$, corresponding to the BEC limit. When E_b increases from 0 to ∞, the system evolves continuously from a BCS superfluid to a BEC of molecules.

The SOC for cold atoms can be generated by the interaction between atoms and laser beams, as shown in many previous literatures [20], and demonstrated in a recent benchmark experiment [7]. In this paper, we consider only a Rashba type of SOC, and the effects of other types of SOC (e.g. Dresselhaus or the combination of both) can be investigated similarly. For simplicity we consider a uniform Fermi gas and neglect the weak harmonic trap in the 2D plane, whose effects can be incorporated using the local density approximation.

The Hamiltonian for this uniform 2D spin-orbit coupled degenerate Fermi gases can be written as

$$H = H_{\rm F} + H_{\rm I} + H_{\rm soc}, \tag{1}$$

where

$$H_{\rm F} = \sum_{\mathbf{k},\sigma} \zeta_{\mathbf{k}} C^\dagger_{\mathbf{k}\sigma} C_{\mathbf{k}\sigma} \tag{2}$$

is the single atom Hamiltonian, $C^\dagger_{\mathbf{k}\sigma}$ is the creation operator for a Fermi atom with the momentum $\mathbf{k} = (k_x, k_y)$, $\sigma = \uparrow, \downarrow$ are the pseudospins of atoms. $\zeta_{\mathbf{k}} = \epsilon_{\mathbf{k}} - \mu$ with the kinetic energy $\epsilon_{\mathbf{k}} = k^2/2m$, the chemical potential μ, and the atom mass m. Henceforth, we take the Planck constant $\hbar = 1$. The s-wave scattering interaction between atom

$$H_{\rm I} = g \sum_{\mathbf{k}} C^\dagger_{-\mathbf{k}\uparrow} C^\dagger_{\mathbf{k}\downarrow} C_{\mathbf{k}\downarrow} C_{-\mathbf{k}\uparrow}, \tag{3}$$

where g is the effective scattering interaction parameter. In a 2D Fermi gas,

$$\frac{1}{g} = -\sum_{\mathbf{k}} \frac{1}{(2\epsilon_{\mathbf{k}} + E_b)}. \tag{4}$$

The Hamiltonian for the Rashba type of SOC for atoms can be written as

$$H_{\rm soc} = \alpha \sum_{\mathbf{k}} [(k_y + ik_x) C^\dagger_{\mathbf{k}\uparrow} C_{\mathbf{k}\downarrow} + (k_y - ik_x) C^\dagger_{\mathbf{k}\downarrow} C_{\mathbf{k}\uparrow}], \tag{5}$$

where α is the SOC strength. In solid state materials, α is generally much smaller than $K_F/(2m)$ with K_F as the Fermi vector. However, in ultra-cold neutral atoms, α can reach the order of $K_F/(2m)$ [20]. Such strong SOC, together with tunable interactions through the Feshbach resonance, may yield some exotic many-body phenomena that have not been explored in solid state systems. Recently, a generalized SOC with the Rashba and the Dresselhaus terms in the Hamiltonian (1) has been considered [11].

III. MEAN FIELD GAP AND ATOM NUMBER EQUATIONS

As the first step for the eventual understanding of the 2D spin-orbit coupled Fermi gas, we consider the zero temperature superfluid physics under the mean field approximation [16]. Generally, the mean field approximation can give qualitatively but not quantitatively correct results [21]. In the mean field approximation, the superfluid order parameter is taken as

$$\Delta = g \sum_{\mathbf{k}} \langle C_{\mathbf{k}\downarrow} C_{-\mathbf{k}\uparrow} \rangle . \tag{6}$$

With this pairing order parameter, we can rewrite the two-body interaction Hamiltonian (3) as

$$H_{\rm I} = -\Delta^2/g + \Delta \sum_{\mathbf{k}} (C_{\mathbf{k}\downarrow} C_{-\mathbf{k}\uparrow} + C^{\dagger}_{-\mathbf{k}\uparrow} C^{\dagger}_{\mathbf{k}\downarrow}). \tag{7}$$

Therefore the total Hamiltonian can be rewritten as

$$H_{\rm B} = \frac{1}{2} \sum_{\mathbf{k}} \Psi^{\dagger}(\mathbf{k}) M_{\mathbf{k}} \Psi(\mathbf{k}) - \frac{\Delta^2}{g} + \sum_{\mathbf{k}} \zeta_{\mathbf{k}} \tag{8}$$

under the Nambu spinor basis $\Psi(\mathbf{k}) = (C_{\mathbf{k}\uparrow}, C_{\mathbf{k}\downarrow}, C^{\dagger}_{-\mathbf{k}\downarrow}, -C^{\dagger}_{-\mathbf{k}\uparrow})^T$, where Bogoliubov-de-Gennes operator

$$M_{\mathbf{k}} = \begin{pmatrix} \zeta_{\mathbf{k}} & \alpha k_+ & \Delta & 0 \\ \alpha k_- & \zeta_{\mathbf{k}} & 0 & \Delta \\ \Delta & 0 & -\zeta_{\mathbf{k}} & -\alpha k_+ \\ 0 & \Delta & -\alpha k_- & -\zeta_{\mathbf{k}} \end{pmatrix} \tag{9}$$

preserves the particle-hole symmetry, $k_{\pm} = k_y \pm i k_x$.

The quasiparticle excitation spectrum

$$E^{\lambda}_{\mathbf{k},\pm} = \lambda \sqrt{(\epsilon_{\mathbf{k}} - \mu \pm \alpha k)^2 + \Delta^2} \tag{10}$$

is the eigenvalue of the matrix $M_{\mathbf{k}}$, $\lambda = \pm$ correspond to the particle and hole branches of the spectrum. For each branch, there are two different excitations due to the existence of the SOC. From Eq. (8), we see the total ground-state energy is

$$E_G = -\frac{\Delta^2}{g} + \sum\nolimits_{\mathbf{k}} [\zeta_{\mathbf{k}} - \frac{1}{2}(E^{+}_{\mathbf{k},+} + E^{+}_{\mathbf{k},-})]. \tag{11}$$

Without the SOC, the term $(E^{+}_{\mathbf{k},+} + E^{+}_{\mathbf{k},-})/2$ reduces to the well-known form

$$E_{\mathbf{k}} = \sqrt{(\epsilon_{\mathbf{k}} - \mu)^2 + \Delta^2}. \tag{12}$$

in the BCS theory.

The ground-state properties of the 2D spin-orbit coupled Fermi gases can be obtained from the atom number equation

$$n = -\frac{\partial E_G}{\partial \mu} = \sum\nolimits_{\mathbf{k}} [1 + \frac{1}{2}(\frac{\partial E^{+}_{\mathbf{k}+}}{\partial \mu} + \frac{\partial E^{+}_{\mathbf{k}-}}{\partial \mu})], \tag{13}$$

and the superfluid gap equation

$$\frac{\partial E_G}{\partial \Delta} = \sum_{\mathbf{k}} [\frac{\Delta}{2\epsilon_{\mathbf{k}} + E_b} - \frac{1}{4}(\frac{\partial E^{+}_{\mathbf{k}+}}{\partial \Delta} + \frac{\partial E^{+}_{\mathbf{k}-}}{\partial \Delta})] = 0. \tag{14}$$

IV. GROUND STATE PROPERTIES

A. Numerical results

We numerically solve the above atom number equation (13) and the gap equation (14) self-consistently to obtain various ground state quantities. In Fig. 1, we plot the dependence of the ground state quantities: the chemical potential μ, the superfluid order parameter Δ, and the ground state energy per atom $E = E_G/n$, on the physical parameters: the SOC strength α and the binding energy E_b. We see that the chemical potential μ decreases with the increasing spin-orbit coupling strength α. With increasing binding energy, the chemical potential also decreases, signaling the crossover physics from the BCS superfluids to the BEC molecules. One interesting feature shown in Fig. 1(a2) is that the shift of the chemical potential induced by the SOC depends only on the SOC strength.

In Fig. 1(b1), we see the superfluid order parameter Δ increases with increasing α. Here Δ_0 is the superfluid order parameter without SOC. For a small α, the change of Δ/Δ_0 is very small. The growth of Δ becomes significant only when αK_F is large than the Fermi energy E_F.

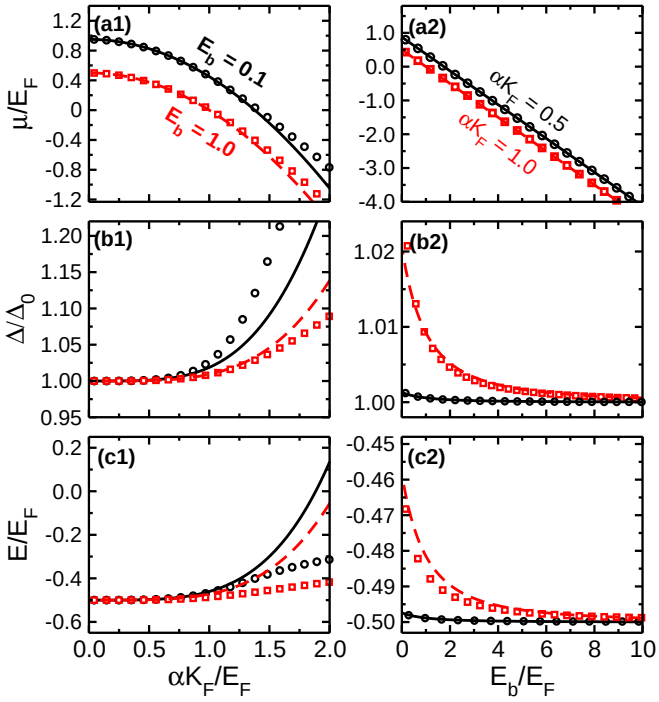

Figure 1: (Color online) (a1-c1) Plot of the chemical potential μ, the dimensionless superfluid pairing gap Δ/Δ_0, and the ground-state energy per atom E with respect to the SOC strength α for the two-body binding energy $E_b = 0.1E_F$ and $1.0\ E_F$. (a2-c2) Plot of μ, Δ/Δ_0, and E with respect to E_b for $\alpha K_F = 0.5E_F$ and $1.0\ E_F$. In all figures, the black solid lines and the red dashed lines represent the approximate analytical results obtained in the paper, while the open symbols correspond to the exact numerical results.

Furthermore, the effects of the SOC are clearly seen for a small E_b (the BCS side), but not important for a large E_b (the BEC side).

The ground state energy per atom E has a similar behavior as Δ/Δ_0. It increases with α, but the growth is only important for a large α. Without SOC $E=-\frac{1}{2}E_F$, and the SOC induces a small correction. The change of E is significant in the BCS side (small E_b), but negligible in the BEC side (large E_b). We note that similar changes of the chemical potential and the superfluid order parameter have been observed numerically in a 3D spin-orbit coupled Fermi gases. All these numerical observed phenomena will be explained in the next subsection where the analytic expressions for these ground state quantities are derived.

B. Analytic results

Although the above numerical results give the dependence of the ground state quantities on the SOC strength for certain parameters, analytic results are desired for a better understanding of the underlying physics. In the following, we present a perturbative method (with α as the small parameter) to analytically extract the fundamental ground-state properties of the spin-orbit coupled Fermi gases. For this purpose, we rearrange Eq. (11) into two parts

$$E_G = E_0 + E_{\rm soc} \tag{15}$$

with

$$E_0 = -\frac{\Delta^2}{g} + \sum\nolimits_{\mathbf{k}}(\zeta_{\mathbf{k}} - E_{\mathbf{k}}) \tag{16}$$

as the ground-state energy without SOC. For a 2D Fermi gas, E_0 can be obtained exactly, yielding [16]

$$E_0 = \frac{m}{4\pi}[\Delta^2 \ln(\frac{\sqrt{\mu^2+\Delta^2}-\mu}{E_b}) - \mu(\sqrt{\mu^2+\Delta^2}+\mu) - \frac{\Delta^2}{2}]. \tag{17}$$

The second term in Eq. (15) is given by

$$E_{\rm soc} = \sum\nolimits_{\mathbf{k}}[E_{\mathbf{k}} - \frac{1}{2}(E^+_{\mathbf{k},+} + E^+_{\mathbf{k},-})], \tag{18}$$

which describes the contribution from the SOC.

Because it is difficult to derive a simple analytic expression for $E_{\rm soc}$ directly, we first perform a Taylor expansion with respect to the SOC strength, and then do the summation over $\mathbf{k}$. Formally, $E_{\rm soc}$ can be written as

$$E_{\rm soc} = \frac{m}{4\pi} C_i(\mu,\Delta)\eta^i \tag{19}$$

with $\eta = m\alpha^2/2$. The coefficients $C_i(\mu,\Delta)$ can be obtained, in principle, for any order. Here, we only give the first six orders

$$C_1 = -4(\sqrt{\mu^2+\Delta^2}+\mu), \tag{20}$$

$$C_2 = -\frac{8}{3}(1+\frac{\mu}{\sqrt{\mu^2+\Delta^2}}), \tag{21}$$

$$C_3 = \frac{-16\Delta^2}{15(\mu^2+\Delta^2)^{3/2}}, \tag{22}$$

$$C_4 = \frac{32\mu\Delta^2}{35(\mu^2+\Delta^2)^{5/2}}, \tag{23}$$

$$C_5 = \frac{64\Delta^2(\Delta^2-4\mu^2)}{315(\mu^2+\Delta^2)^{7/2}}, \tag{24}$$

$$C_6 = \frac{-128\mu\Delta^2(3\Delta^2-4\mu^2)}{693(\mu^2+\Delta^2)^{9/2}}. \tag{25}$$

Although the expression for $E_{\rm soc}$ is very complicate, the expressions for the chemical potential μ and the superfluid pairing order Δ are very simple, as we will show later in the paper. With the ground-state energy E_G, the superfluid pair order and the chemical potential can be derived by self-consistently solving the corresponding gap and number equations

$$\ln(\frac{\sqrt{\mu^2+\Delta^2}-\mu}{E_b}) = G_\Delta(\eta,\Delta,\mu), \tag{26}$$

$$\sqrt{\mu^2+\Delta^2}+\mu = 2E_F - G_\mu(\eta,\Delta,\mu) \tag{27}$$

analytically, where $G_\Delta(\eta,\Delta,\mu) = \sum_i \frac{\partial C_i(\mu,\Delta)}{\partial\Delta}\eta^i$, and $G_\mu(\eta,\Delta,\mu) = \sum_i \frac{\partial C_i(\mu,\Delta)}{\partial\mu}\eta^i$. E_F is the Fermi energy for a 2D non-interacting Fermi gas without SOC and with the density $n = mE_F/\pi$. Without SOC ($\eta=0$), $G_\Delta(\eta,\Delta,\mu) = G_\mu(\eta,\Delta,\mu) = 0$, and Eqs. (26) and (27) become

$$\sqrt{\mu^2+\Delta^2}-\mu = E_b,$$
$$\sqrt{\mu^2+\Delta^2}+\mu = 2E_F.$$

In this case, the superfluid pairing order and the chemical potential are given exactly by $\Delta_0 = \sqrt{2E_bE_F}$ and $\mu_0 = E_F - E_b/2$ [16], as expected.

In the presence of SOC ($\eta \neq 0$), the nonlinear equations (26) and (27) cannot be solved exactly. However, approximate solutions can be derived for the physical parameters within current experimentally achievable region. Since the ground-state energy depends on Δ^2, the solutions of Eqs. (26) and (27) can be assumed to be $\mu = \sum_{i=0}\mu_i\eta^i$ and $\Delta^2 = \sum_{i=0}\Lambda_i\eta^i$. Substituting these expressions into the nonlinear equations (26) and (27) and then comparing the coefficients for the same order of η^i, we obtain Λ_i and μ_i respectively.

1. *Chemical potential*

After a straightforward but tedious calculation, the coefficients for the chemical potential are given by $\mu_1 =$

-2, $\mu_2 = 4E_b/[3(E_b+2E_F)^2]$ and $\mu_3 = -64E_b(E_b - 4E_F)/[15(E_b+2E_F)^4]$. Note that the second order μ_2 is already very small for all different values of E_b when $\eta < E_F$, therefore the high-order terms do not affect the chemical potential significantly. The chemical potential can then be written as

$$\mu \simeq E_F - \frac{E_b}{2} - 2\eta. \tag{28}$$

From Fig. 1a, we see Eq. (28) agrees well with the exact values of the chemical potential obtained from numerically solving Eqs. (13) and (14) self-consistently.

Equation (28) shows clearly that with the increasing SOC strength α, the chemical potential μ is decreased by $2\eta = m\alpha^2$, as shown in Fig. 2. If we define an effective chemical potential $\overline{\mu} = \mu + 2\eta = \mu + m\alpha^2$, Eq. (28) can be rewritten as $\overline{\mu} = E_F - E_b/2$. Similar to the previous discussion without SOC, we find that in the asymptotic BCS limit with a weak bound state ($E_b \ll E_F$), the chemical potential $\overline{\mu} \simeq E_F$. However, in the deep BEC regime with a strong bound state ($E_b \gg E_F$), the chemical potential $\overline{\mu} = -E_b/2$. The BCS-BEC crossover may occur around the crossover point $\overline{\mu} = 0$ [16]. Furthermore, in the presence of SOC, Eq. (28) can also be written as $\mu = \mu_f + \mu_\Delta$, where $\mu_f = E_F - 2\eta$ is the chemical potential for the free Fermi gas and $\mu_\Delta = -E_b/2 + \sum_{i=1} \mu_{\Delta i}(E_b)\eta^i$ reflects the revision of the chemical potential induced by the two-body binding energy E_b. Here $\mu_{\Delta 1} = 0$ implies that the binding energy E_b has no effect on the chemical potential μ at the order of $\eta = m\alpha^2/2$.

It is important to point out that although the chemical potential μ only has a simple shift from that without SOC, the underlying physics is quite different. Without SOC, the pairing wave function is simply singlet. However, in the presence of SOC, each energy band contains both spin up and down components. As a result, the pairing wave function has a more complicated structure with both singlet and triplet components [22]. The triplet pairing correlations in s-wave superfluids may be used to detect the anisotropic Fulde-Ferrell-Larkin-Ovchinikov states [23]. In addition, the 2D Fermi gases with SOC can exhibit p-wave character in the helicity bases. If a Zeeman field in Hamiltonian (8) is added, a novel topological phase transition from non-topological superfluids to topological superfluids can be induced. In the topological superfluid phase, there exist Majorana fermions and the associated non-Abelian statistics, which are the critical ingredients for implementing topological quantum computing [18].

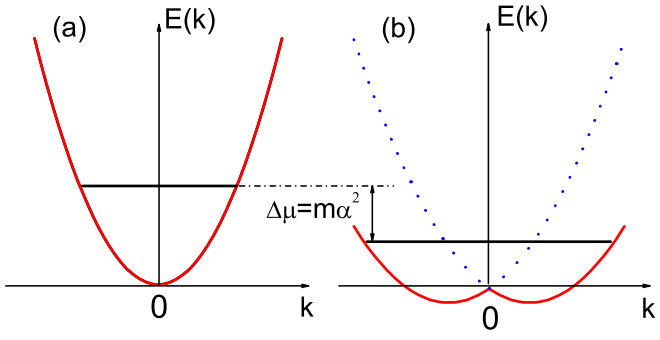

Figure 2: (Color online) (a) The chemical potential without SOC in the BCS limit. (b) The chemical potential with SOC in the BCS limit. For weak SOC, their difference $\Delta\mu = m\alpha^2$.

2. *Superfluid order gaps*

The effects of SOC are more interesting for the superfluid pairing gap Δ. Applying the same procedure as that for the chemical potential, we find

$$\Delta^2 \simeq 2E_bE_F + \frac{16E_bE_F}{3(E_b+2E_F)^2}\eta^2. \tag{29}$$

There is no first-order correction with respect to η ($\sim \alpha^2$) for Δ^2, and the second-order η^2 ($\sim \alpha^4$) is the leading correction. Moreover, the second-order coefficient $\partial^2\Delta^2/\partial\eta^2$ is always positive and has a maximum $4\eta^2/3$ ($= m^2\alpha^4/3$) when $E_b = 2E_F$. The high-order coefficients for η^3 and η^4 are $\Lambda_3 = -512E_bE_F(E_b - E_F)/[15(E_b+2E_F)^4]$ and $\Lambda_4 = 64E_bE_F(1017E_b^2 - 3508E_bE_F + 1076E_F^2)/[315(E_b+2E_F)^6]$ respectively.

In order to see the effect of SOC on the superfluid pairing gap more clearly, we introduce a dimensionless quantity

$$\Delta_d = \frac{\Delta}{\Delta_0} \simeq \sqrt{1 + \frac{8}{3(E_b+2E_F)^2}\eta^2}, \tag{30}$$

where Δ_0 is the superfluid pairing gap without SOC. In the asymptotic BCS limit with a weak bound state ($E_b \ll E_F$), $\Delta_d \simeq \sqrt{1+2\eta^2/E_F^2}$. For a weak SOC ($\eta \ll E_F$) in typical solid-state materials, $\Delta_d \simeq 1$, which means that the SOC does not affect the superfluid pairing gap significantly. However, for a strong SOC $\eta \sim E_F$ that has been achieved for ultracold atoms [7], this gap can be enhanced greatly. In the deep BEC regime with a strong binding energy ($E_b \gg E_F$ and $E_b \gg \eta$), $\Delta_d \simeq \sqrt{1+8\eta^2/(3E_b^2)}$, therefore the superfluid pairing gap increases only slightly with the increasing SOC strength. These analytic results agree well with the numerical results shown in Fig. 1b. Note that similar behavior for Δ_d is also observed in the numerical results in 3D [10].

3. *Ground-state energy per atom*

In terms of Eqs. (28) and (29), the ground-state energy per Fermi atom $E = E_G/n$ can be obtained

$$E \simeq -\frac{1}{2}E_F + \frac{8E_F}{3(E_b+2E_F)^2}\eta^2. \tag{31}$$

The comparison of Eq. (31) with the direct numerical simulation results is shown in Fig. 1c. The ground-state energy, like the superfluid pairing gap, depends on η^2 ($\sim \alpha^4$). In the asymptotic BCS limit ($E_b \ll E_F$), $E \simeq -E_F/2+2\eta^2/(3E_F)$, which means that the ground-state energy can be enhanced significantly only for a large η. In the deep BEC regime ($E_b \gg E_F$ and $E_b \gg \eta$), $E \simeq -E_F/2 + 8E_F\eta^2/(3E_b^2)$, therefore the ground-state energy only increases slightly even when $\eta \sim E_F$. In addition, the high-order coefficients for η^3 and η^4 are given by $E_3 = -128E_bE_F/[5(E_b + 2E_F)^4]$ and $E_4 = 128E_bE_F(491E_b - 538E_F)/[315(E_b + 2E_F)^6]$ respectively. Note that although such mean field theory gives qualitatively correct results, it may not agree quantitatively with the experimental results in the deep BEC regime as shown in recent Monte Carlo numerical simulation for the 2D Fermi gases without SOC [21].

Finally, we want to remark that if the high-order terms in the chemical potential μ, the superfluid pairing gap Δ, and the ground-state energy per Fermi atom $E = E_G/n$ are included, the analytical results in Eqs. (28), (30) and (31) fit better with the numerical results even for $E_F < \alpha K_F < 3.0E_F$.

V. DISCUSSION AND CONCLUSION

The mean field zero temperature BCS-BEC crossover physics discussed above provides the first critical step towards the understanding of the 2D spin-orbit coupled degenerate Fermi gases. Clearly, many issues need be further explored in the future, as demonstrated by the development along this direction after the initial submission of our paper. In particular, the finite temperature effect need be taken into account in a realistic experiment. Without SOC, it is known that there are no superfluids for 2D degenerate Fermi gas at a finite temperature [24], where relevant physics is the Berezinskii-Kosterlitz-Thouless (BKT) transition [25], leading to the generation of the vortex-antivortex pairs. Recent some interesting effects of the SOC on the BKT transition [26] has been investigated. In experiments, the Fermi gases are confined in a 2D harmonic trap, whose effects may be taken into account using the local density approximation, as shown in the recent preprint [26]. The trap geometry for the Fermi gases may also be quais-2D instead of the strict 2D. In this case, the confinement along the third direction may affect the critical transition temperature, which need be further explored.

In summary, motivated by the recent experimental breakthrough for the realization of the SOC for cold atoms and the 2D degenerate Fermi gas, we investigate the zero temperature BCS-BEC crossover physics in 2D spin-orbit coupled degenerate Fermi gases using the mean field approximation. By solving the corresponding gap and atom number equations both numerically and analytically, we reveal the ground state properties of the spin-orbit coupled 2D Fermi gases. Our analytic results agree quantitatively with our numerical results in 2D and qualitatively with previous numerical results for the 3D spin-orbit coupled Fermi gases, where analytic results are lacked. The analytic expressions for various physical quantities may provide a powerful tool for engineering and probing many new topological phenomena in 2D Fermi gases, including the intriguing Majorana physics and the associated non-Abelian statistics.

Acknowledgments

We thank Yongping Zhang, Li Mao, and Wei Yi for helpful discussion. This work is supported by DARPA-YFA (N66001-10-1-4025), ARO (W911NF-09-1-0248), NSF (PHY-1104546), and AFOSR (FA9550-11-1-0313). GC is also supported by the 973 program under Grant No. 2012CB921603, the NNSFC under Grant No. 11074154, and the ZJNSF under Grant No. Y6090001.

[1] N. Nagaosa, J. Sinova, S. Onoda, A. H. MacDonald, and N. P. Ong, Rev. Mod. Phys. **82**, 1539 (2010).

[2] D. Xiao, M. -C. Chang, and Q. Niu, Rev. Mod. Phys. **82**, 1959 (2010).

[3] X. -L. Qi, and S. -C. Zhang, Rev. Mod. Phys. **83**, 1057 (2011)

[4] I. Žutić, J. Fabian, and S. Das Sarma, Rev. Mod. Phys. **76**, 323 (2004).

[5] V. B. Berestetskii, E. M. Lifshitz, and L. P. Pitaevskii, *Quantum electrodynamics*, (Butterworth-Heinemann, 1982).

[6] A. J. Leggett, *Quantum Liquids: Bose condensation and Cooper pairing in condensed-matter systems* (Oxford University Press Inc., New York, 2006).

[7] Y. -J. Lin, K. Jiménez-García, and I. B. Spielman, Nature (London) **471**, 83 (2011); Y. -J. Lin, R. L. Compton1, K. Jiménz-García, J. V. Porto, and I. B. Spielman, Nature (London) **462**, 628 (2009).

[8] C. Wang, C. Gao, C. -M. Jian, and H. Zhai, Phys. Rev. Lett. **105**, 160403 (2010); T.-L. Ho and S. Zhang, Phys. Rev. Lett. **107**, 150403 (2011); Y. Zhang, L. Mao, and C. Zhang, arXiv:1102.4045; H. Hu, H. Pu, and X.-J.Liu, arXiv: 1108.4233.

[9] S. K. Yip, Phys. Rev. A **83**, 043616, (2011); Z. F. Xu, R. Lü, and L. You, Phys. Rev. A **83**, 053602 (2011); T. Kawakami, T. Mizushima, and K. Machida, Phys. Rev. A **84**, 011607(R) (2011); C. Jian and H. Zhai, Phys. Rev. B **84**, 060508 (2011); C. Wu, I. Mondragon-Shem, and X.-F. Zhou, Chin. Phys. Lett. **28**, 097102 (2011).

[10] J. P. Vyasanakere, S. Zhang, and V. B. Shenoy, Phys. Rev. B **84**, 014512 (2011); M. Gong, S. Tewari, and C. Zhang, Phys. Rev. Lett. **107**, 195303 (2011); Z. -Q. Yu, and H. Zhai, Phys. Rev. Lett. **107**, 195305 (2011); H. Hu, L. Jiang, X. -J. Liu, and H. Pu, Phys. Rev. Lett. **107**, 195304 (2011); M. Iskin, and A. L. Subasi, Phys. Rev. Lett. **107**, 050402 (2011); Phys. Rev. A **84**, 041610 (R) (2011); Phys. Rev. A **84**, 043621 (2011); W. Yi, and G. -C. Guo, Phys. Rev. A **84**, 031608 (2011); L. Han, and

C. A. R. Sá de Melo, arXiv:1106.3613.
[11] L. Dell'Anna, G. Mazzarella, and L. Salasnich, Phys. Rev. A **84**, 033633 (2011).
[12] D. S. Petrov, M. Holzmann, and G. V. Shlyapnikov, Phys. Rev. Lett. **84**, 2551 (2000); S. S. Botelho, and C. A. R. Sá de Melo, Phys. Rev. Lett. **96**, 040404 (2006); W. Zhang, G. -D. Lin, and L. -M. Duan, Phys. Rev. A **77**, 063613 (2008); Phys. Rev. A **78**, 043617 (2008); I. Bloch, J. Dalibard, and W. Zwerger, Rev. Mod. Phys. **80**, 885 (2008).
[13] K. Martiyanov, V. Makhalov, and A. Turlapov, Phys. Rev. Lett. **105**, 030404 (2010).
[14] B. Fröhlich, M. Feld, E. Vogt, M. Koschorreck, W. Zwerger, and M. Köhl, Phys. Rev. Lett. **106**, 105301 (2011).
[15] C. Chin, R. Grimm, P. Julienne, and E. Tiesinga, Rev. Mod. Phys. **82**, 1225 (2010).
[16] M. Randeria, J. -M. Duan, and L. -Y. Shieh, Phys. Rev. Lett. **62**, 981 (1989); Phys. Rev. B **41**, 327 (1990).
[17] S. Sachdev, Science **288**, 475 (2000); S. E. Korshunov, Phys. Usp. **49**, 225 (2006).
[18] S. Tewari, S. Das Sarma, C. Nayak, C. Zhang, and P. Zoller, Phys. Rev. Lett. **98**, 010506 (2007); C. Zhang, S. Tewari, R. M. Lutchyn, and S. Das Sarma, Phys. Rev. Lett. **101**, 160401 (2008); C. Nayak, S. H. Simon, A. Stern, M, Freedman, and S. D. Sarma, Rev. Mod. Phys. **80**, 1083 (2008).
[19] J. Tempere, M. Wouters, and J. T. Devreese, Phys. Rev. B **75**, 184526 (2007).
[20] J. Ruseckas, G. Juzeliūnas, P. Öhberg, and M. Fleischhauer, Phys. Rev. Lett. **95**, 010404 (2005); T. D. Stanescu, C. Zhang, and V. Galitski, Phys. Rev. Lett. **99**, 110403 (2007); C. Zhang, Phys. Rev. A **82**, 021607(R) (2010); G. Juzeliūnas, J. Ruseckas, and J. Dalibard, Phys. Rev. A **81**, 053403 (2010); J. D. Sau, R. Sensarma, S. Powell, I. B. Spielman, and S. Das Sarma, Phys. Rev. B **83**, 140510 (2011); D. L. Campbell, G. Juzeliūnas, and I. B. Spielman, Phys. Rev. A **84**, 025602 (2011). J. Dalibard, F. Gerbier, G. Juzeliunas, and P. Ohberg, Rev. Mod. Phys. (accepted for publications)
[21] G. Bertaina, and S. Giorgini, Phys. Rev. Lett. **106**, 110403 (2011).
[22] L. P. Gor'kov, and E. I. Rashba, Phys. Rev. Lett. **87**, 037004 (2001).
[23] I. Zapata, F. Sols, and E. Demler, arXiv:1106.1605.
[24] P. C. Hohenberg, Phys. Rev. **158**, 383 (1967).
[25] V. L. Berezinskii, Sov. Phys. JETP **32**, 493 (1971); J. M. Kosterlitz and D. Thouless, J. Phys. C **5**, L124 (1972).
[26] L. He, and X. -G. Huang, arXiv:1109.5577.